

Intense pulsed laser irradiation of bulk crystal

C. FLOREA, M. ZAMFIRESCU^a, F. JIPA^a, A. VELEA^b

ESIEE Engineering, Université Paris - Est, France

^a*National Institute R&D for Lasers, Plasma and Radiation Physics, P.O. Box MG. 5, Magurele-Ilfov, Romania*

^b*National Institute R&D of Materials Physics, Bucharest-Magurele, P.O. Box, Mg. 7, Romania*

The paper describes the effects of pulsed laser irradiation on a solid bulk crystal. New approach is developed, which comprises the RPE-type resonant signals obtained from the conduction of the electrons of Ca metal and the hydrogen centers, that are defects induced by irradiation in a CaF₂ sample.

(Received March 10, 2011; accepted March 24, 2011)

Keywords: RPE, Laser irradiation, Bulk crystal, CaF₂

1. Introduction

The interaction of laser beam with the solid matter is of great interest with the advent of high power lasers. The application of the Extreme Light Infrastructure (ELI) will open the way towards a new advanced physics in the field of interaction between the intense light and the matter in its condensed state.

The methods L.I.P.S. (Laser Induced Plasma Spectroscopy) or L.I.B.S. (Laser Induced Breakdown Spectroscopy) are largely used in order to characterize the plasma formation, the laser beams and the targets.

We add a new approach which comprises the RPE-type resonant signals obtained from the conduction of the electrons of metal Ca and the hydrogen centers defects induced by light irradiation in a CaF₂ sample.

2. Laser interaction with matter

The characteristic of laser-solid material interaction depends on many parameters including fluence regime and material structure. We tried to discuss the interaction between the energetic photon beam with bulk crystal as a function of the energy pulse level. In Fig. 1 are presented the three regimes of laser –solid interaction: low flow regime, middle flow regime and high flow regime. Some characteristic of these regimes are presented shortly and the plasma plume development is discussed.

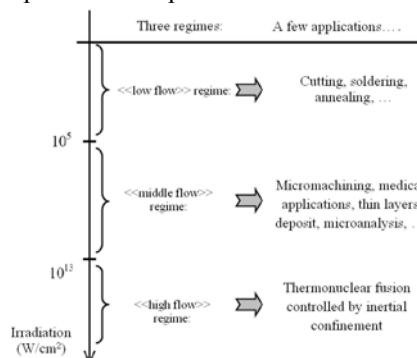


Fig. 1. The current domains of the laser irradiation.

The development of plasma during interaction is shown in Fig. 2 for the case of CaF₂ as compared with the plasma development in air. The plasma expansion is shown as a function of time.

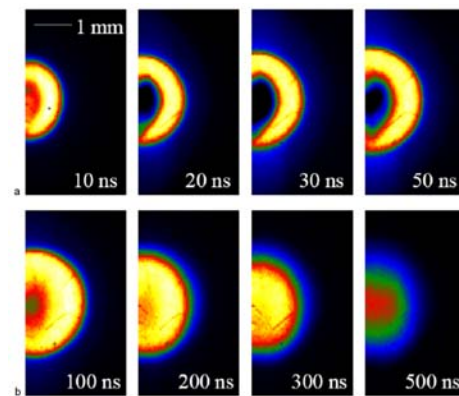


Fig. 2. (a) Plasma at CaF₂; (b) Plasma in air.

The stages of plasma formation during irradiation of a solid target are shown in Fig. 3. Firstly by absorption of the laser pulse energy the temperature increases (a), then fusion is produced and an interface plasma-solid is formed and slowly moved in the solid (b). In the third stage (c) matter emission takes place. This process is well known as ablation process. Finally (stage d), plasma plume is produced.

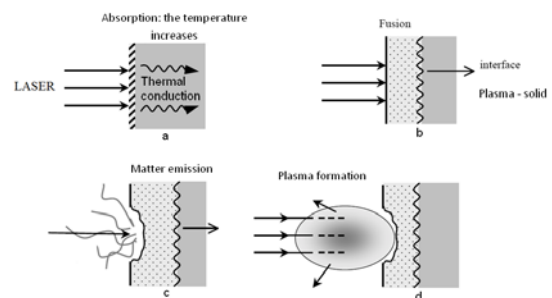


Fig. 3. Formation stages of plasma during a laser irradiation/solid target.

The interaction of the “heavy” particles present in the plasma created by laser pulse during the interaction with a CaF_2 single crystal target is illustrated in Fig. 4.

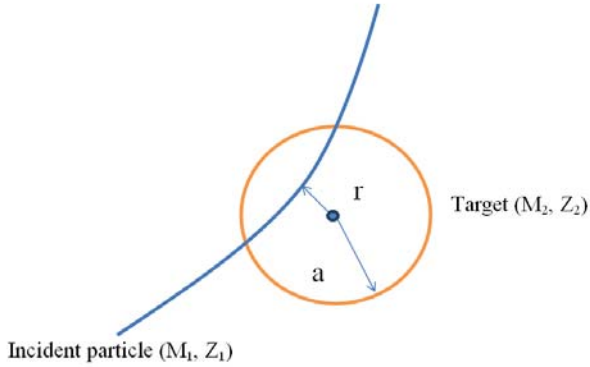


Fig. 4. Sketch of the interaction of a heavy particle with the plasma created by the laser pulse.

The (M_1, Z_1) and (M_2, Z_2) are the masses and the atomic numbers; a = screen radius (Thomas-Fermi radius); E = kinetic energy of the incident particle. The reduced energy ε is then given by:

$$\varepsilon = E \cdot \frac{M_2}{\frac{M_1 + M_2}{Z_1 \cdot Z_2} a}$$

where $a = 0.885 \cdot a_0 \cdot \left(\frac{2}{Z_1^3} + \frac{2}{Z_2^3} \right)^{\frac{1}{2}}$ with

$$a_0 = \frac{\hbar^2}{m e_0^2} = \frac{1}{\alpha} \cdot \tilde{\lambda}_C \approx 0.529177 \times 10^{-10} m \text{ (Bohr radius)}$$

We define the energy loss by nuclear shocks by length unit (named nuclear stop power) such as:

$$\left(-\frac{dE}{dx} \right)_n = N \int_0^{T_{\max}} T \cdot \frac{d\sigma(E, T)}{dT} \cdot dT$$

where:

- E is the energy of the incident particle.
- N is the atomic density of the target.
- T is the energy transferred to target core. It has a maximum value T_{\max} when the binary collision is frontal ($T_{\max} = 4 \cdot \frac{M_1 \cdot M_2}{(M_1 + M_2)^2} \cdot E$),

- $d\sigma(E, T)$ is the differential efficient section of the collision.

In order to calculate the nuclear stop power $\left(-\frac{dE}{dx} \right)_n$, we must know the differential efficient section of the colliding $d\sigma(E, T)$.

3. The irradiation effects

The first experimental observations (Montpreville [1], Johnson and Chaderton [2], Hughes and Jain [3]) have shown the formation in an initial network of colloids, homothetic with that of fluorine ions of the crystal. The diameter of a colloidal particle is about 100 Å. We consider the colloidal particles as inclusions of rectangular shape. Their stopping path has a length between 300 and 1000 Å.

In the case of our experiences, the beam energy is higher (going up to MeV). The samples are CaF_2 single crystals of rectangular shape (with length of 1 cm, width of 1 mm and thickness of 100 μm). The energies of the radiations are in the range going from keV up to MeV values. The losses of one charged particle were estimated (Fig. 5).

The first experimental results which were obtained prove the formation of the colored centers that foreshadow o colloidal formation. We have tried to understand the evolution of the metal colloidal particle formation of Ca in CaF_2 (Fig. 6).

The modified Montpreville equation solution simulation took into consideration the evolution of the colloids concentration C_c function of the concentration of the F clustered centers – cFagg.

Our calculations give 10^{12} particles by cm^2 and lead to an average beam diameter of 10^{-6} cm, a value in very good agreement to that experimentally reported (100 Å). The solution of the analytical model for the concentration cFagg was simulated for different values of the irradiation rating GF (GF = the number of excitons by anionic site and by second – Fig. 7 - 9)

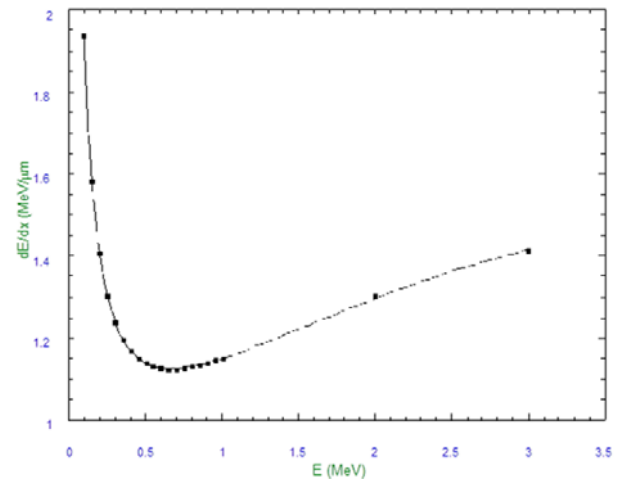


Fig. 5. Energy losses of a charged particles beam in a CaF_2 sample.

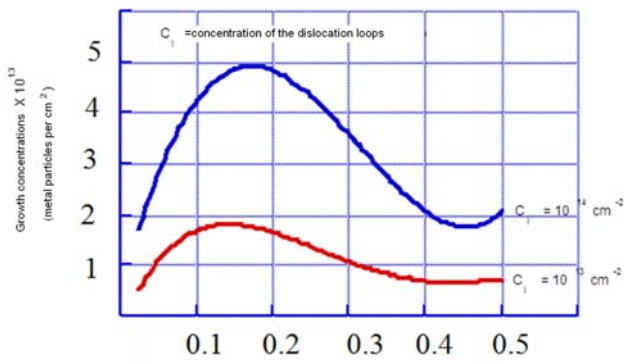


Fig. 6. The concentration of the dislocation loops versus growth concentration.

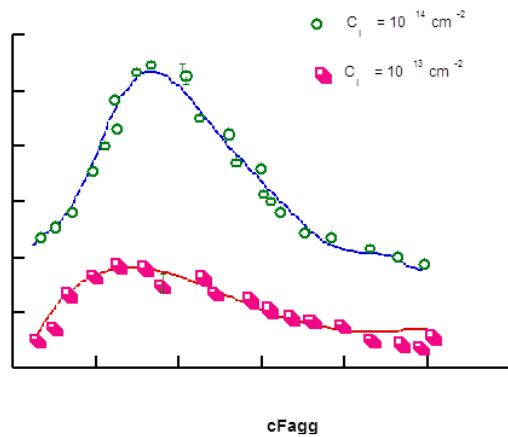


Fig. 7. Theoretical model and experimental data which describe the formation of the centers F. in an irradiated CaF₂; the parameter taken into consideration is the concentration of dislocation curves (Reprint : C. Florea Note Technique CEA, 1991).

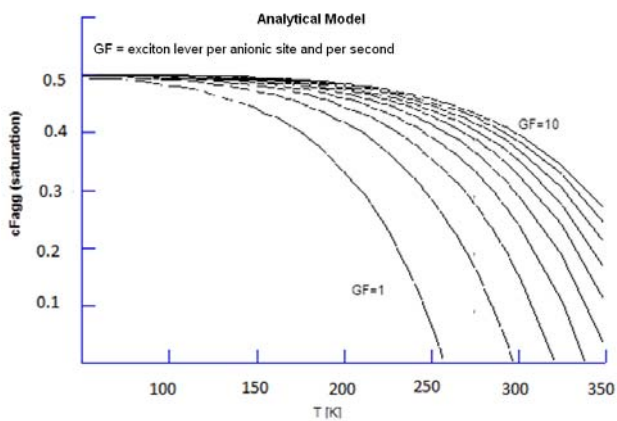


Fig. 8. Concentration of the F clustered centers – cF_{agg} versus temperature.

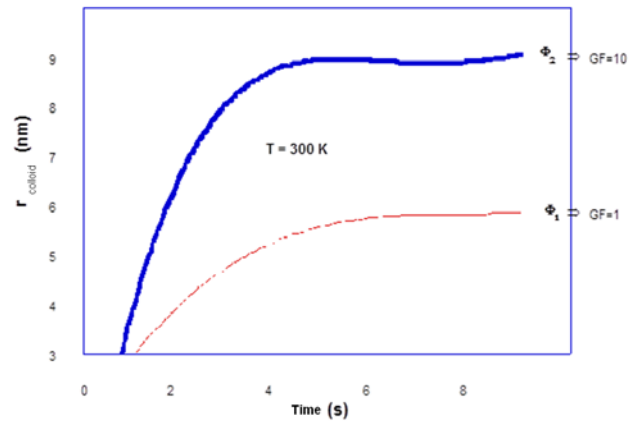


Fig. 9. The radius of the colloid particle versus time.

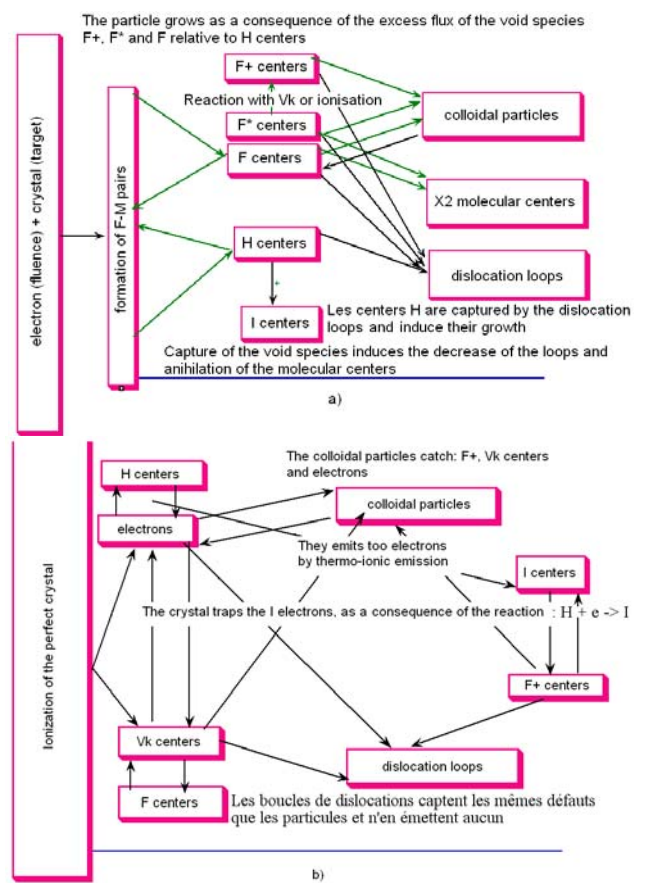


Fig. 10. The schematic of the reactions: (a) The lattice defects and their main reactions (b) The charged defects and their main reactions.

4. Discussion

An arranged population of “cavities” in the CaF₂ fluorine subnet develops under irradiation. The swelling of the materials is less important when the cavities are arranged. Thus, it is possible to study the arrangement of these cavities [4-9].

As the cationic subnet remains unchanged, the cavities are similar to the Ca inclusions (Fig. 10). From

now on, we will equally use the two terms: inclusion or cavity.

The origin of the inclusions is applied to the radiolysis phenomenon: by a complex mechanism, the anions are ionized and moved from their places, thus there is the occurrence of the H centers. The fluorine atoms (or ions) in interstitial positions, while the origin place is occupied by a loophole that entraps (for stability reasons) an electron. Such a loophole consolidated by electronic capture is a F center [10, 11]. The F centers spread in the crystal. A portion is eliminated on the wells and by recombination with the centers H [12], while another portion agglomerates in clusters the growth of which is directly observed in the electronic microscope.

The evolution of the centers H is less clear. If the behavior of the alkaline-earth halides was similar to those of the alkaline halides, the centers F would be eliminated in the crystal and would form the interstitial loops [12]. The inclusions are spread in an unordered manner and the order appears only progressively during the irradiation. At high temperatures (close to 400 K), the inclusions remain. They have a rectangular shape $\{100\}$ and are distributed randomly in the crystal.

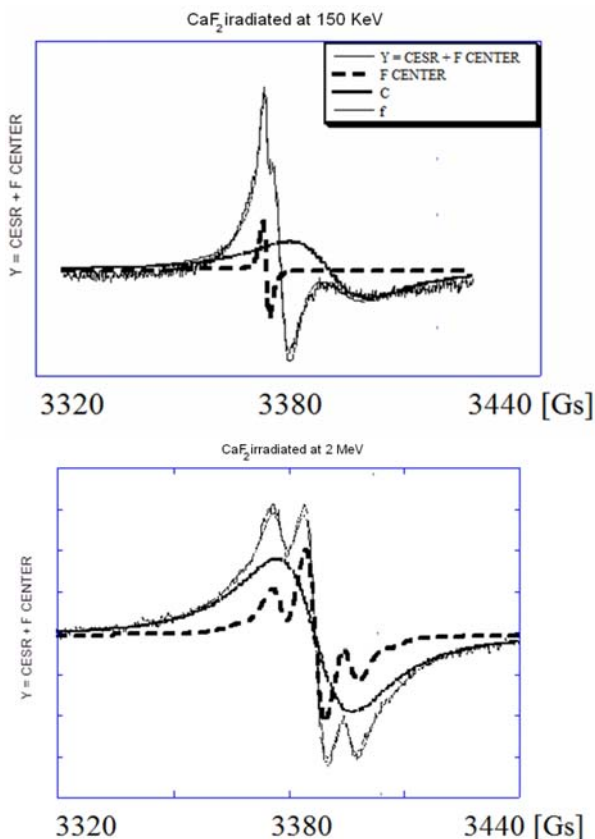


Fig. 11. The signal RES due to conduction electrons and to the centers F; CESR = signal due to conduction electrons; F CENTER = signal due to F centers; fit = smooth signal.

The spectra R.P.E. (Fig. 11) are recorded with the same frequency of 9.46 GHz. The fields are now next to

1000 Gauss. The temperature during the measurements is ~ 4 K. The found values of a diagram $\{g^2 / \sin^2\theta, -\theta$ being the angle between the magnetic field and the crystal axis /in this case: (1,1,1)/for the components of the spectral decomposition tensor $\vec{g}(g_{\parallel}; g_{ortho})$ (for an axial symmetry) can be found in the following table:

COMPONENTS	g_{\parallel}	g_{ortho}
SYMMETRY		
Cubic	6.80	6.80
Tetragonal	7.80	6.25
Trigonal	3.30	8.55

The g found values are very close to those reported by Ranon and Low for the tetragonal specter ($= g_{\parallel}=7.78$, $g_{ortho} = 6.25$) and for the trigonal specter ($g_{\parallel} = 3.30$, $g_{ortho} = 8.54$). We have however, other intensities of the rays, corresponding to the same angular values of the field compared with the axis TZ. In our study, for the non-irradiated sample, the intensities of the signals are found in the relationships T (tetragonal) : t (trigonal) : c (cubic) = 4 : 2 : 3. The spectra recorded do not present any trace of second type (II) tetragonal and trigonal signals named by Ranon and Low.

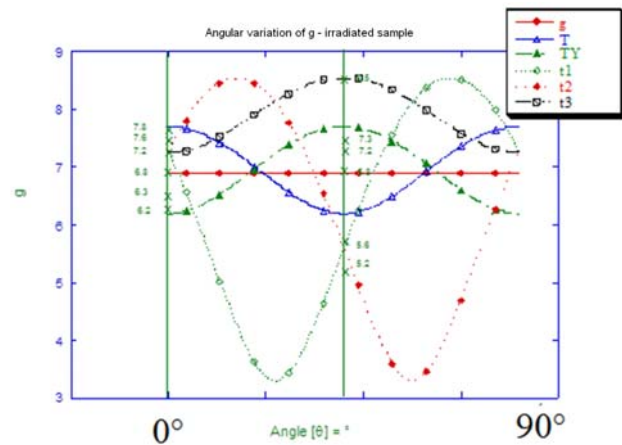


Fig. 12. The angular variation of g in irradiated samples.

The intensities are found in the relationships T : t : c = 8 : 5 : 4. This change of intensities is different enough compared with the result of Ranon and Low. The absence of the type II trigonal rays (rays that grow in intensity at Ranon and Low) is related to the origin of the compensation oxygen which diagonally occupies a site empty of fluorine.

The angular diagrams were built from the recorded spectra (Fig. 12).

5. Conclusions

The comparisons of the spectra in the irradiated samples and the non-irradiated samples allowed us to draw some conclusions:

- the rays preserve their angular variation;
- the intensity of the cubic rays decrease;
- the intensity of the tetragonal rays grows slightly;
- the trigonal rays grow significantly;

We have observed the cubic symmetry change of the F^- ligand network towards a C_{4V} symmetry. The tetragonal change is explained as a result of a load compensation by an interstitial defect created by a F^- ion which occupies the center of the neighboring ligand cube, initially empty, of the CaF_2 network. In the trigonal case, we presume that a O^{2-} ion replaces a F^- ion on one of the peaks of the surrounding fluorine cubical neighbouring.

References

- [1] Ch. T. de Montpreville - Note Technique SRPM 6707 (1985).
- [2] E. Johnson, L. Chaderton, Radiation Effects **79**, 183 (1983).
- [3] A. Hughes, S. Jain, Adv. in Phys. **28**, 717 (1979).
- [4] F. Beuneu, C. Florea, P. Vajda, Radiation Effects and Defects in Solids **136**, 175 (1995).
- [5] V. Lupei, S. Georgescu, V. Florea, IEEE J. Quantum Electronics **29**, 426 (1993).
- [6] S. Georgescu, V. Lupei, C. Hapenciuc, C. Florea, C. Naud, C. Porte, J. of Luminescence **93**, 281 (2001).
- [7] S. Georgescu, O. Toma, C. Florea, C. Naud, J. of Luminescence **101**, 87 (2003).
- [8] C. Florea – Note Technique SESI, CEA, 1991.
- [9] U. Ranon, W. Low, Phys. Rev. **132**, 1609 (1963).
- [10] C. Florea, et al., Numerical Physics, Ed. CREDIS Univ. Bucharest, ISSN 1842-5380, p. 113, 2006.
- [11] C. Florea, Numerical Physics, Ed. CREDIS Univ. Bucharest, ISSN 1842-5380, p. 1, 2006.
- [12] C. Florea, S. Georgescu, Optoelectron. Adv. Mater.– Rapid Comm. **1**(5), 212 (2007).

*Corresponding author: floreac@esiee.fr